Altered synaptic and firing properties of cerebellar Purkinje cells in a mouse model of ARSACS

Visou Ady[1], Brenda Toscano-Márquez[1], Moushumi Nath[1], Philip K. Chang[2], Jeanette Hui[1], Anna Cook[1], François Charron[2], Roxanne Larivière[3], Bernard Brais[3], R. Anne McKinney[2] and Alanna J. Watt[1]

[1]*Department of Biology, McGill University, Montréal, Canada*
[2]*Department of Pharmacology and Therapeutics, McGill University, Montréal, Canada*
[3]*Department of Neurology and Neurosurgery, Montréal Neurological Institute, McGill University, Montréal, Canada*

Edited by: Jaideep Bains & Katalin Toth

Key points

- Autosomal recessive spastic ataxia of Charlevoix–Saguenay (ARSACS) is an early-onset neurodegenerative human disease characterized in part by ataxia and Purkinje cell loss in anterior cerebellar lobules. A knock-out mouse model has been developed that recapitulates several features of ARSACS.
- Using this ARSACS mouse model, we report changes in synaptic input and intrinsic firing in cerebellar Purkinje cells, as well as in their synaptic output in the deep cerebellar nuclei.
- Changes in firing are observed in anterior lobules that later exhibit Purkinje cell death, but not in posterior lobules that do not.
- Our results show that both synaptic and intrinsic alterations in Purkinje cell properties likely contribute to disease manifestation in ARSACS; these findings resemble pathophysiological changes reported in several other ataxias.

Abstract Autosomal recessive spastic ataxia of Charlevoix–Saguenay (ARSACS) is an early-onset neurodegenerative disease that includes a pronounced and progressive cerebellar dysfunction. ARSACS is caused by an autosomal recessive loss-of-function mutation in the *Sacs* gene that encodes the protein sacsin. To better understand the cerebellar pathophysiology in ARSACS, we studied synaptic and firing properties of Purkinje cells from a mouse model of ARSACS, *Sacs*$^{-/-}$ mice. We found that excitatory synaptic drive was reduced onto *Sacs*$^{-/-}$ Purkinje cells, and that Purkinje cell firing rate, but not regularity, was reduced at postnatal day (P)40, an age when ataxia symptoms were first reported. Firing rate deficits were limited to anterior lobules that later display Purkinje cell death, and were not observed in posterior lobules where Purkinje

---

Visou Ady was first introduced to molecular biology and electrophysiology for his Master's project. During his PhD, he combined slice electrophysiology and pharmacology techniques to unravel a novel type of channel–receptor gating mechanism in cerebellar Purkinje cells. Later, in the Watt lab, he studied cerebellar circuit development and cerebellar pathophysiology in a hereditary cerebellar ataxia mouse model. Currently, he works in the Cassanova lab on deciphering the modulation exerted by the pulvinar onto the visual cortical network *in vivo*. **Brenda Toscano-Márquez** received her PhD in Biology from McGill University, studying the action of neuromodulators in the electrosensory system in weakly electric fish. For her postdoctoral research, she joined the Watt lab, where she is using her training in electrophysiology and molecular techniques to studying the pathophysiology that underlies the onset of ARSACS in the hope of gaining better insights into developing treatments for this disease.

V. Ady and B. Toscano-Márquez contributed equally.

R.A.M. and A.J.W. are joint senior and joint corresponding authors.

cells are not lost. Mild firing deficits were observed as early as P20, prior to the manifestation of motor deficits, suggesting that a critical level of cerebellar dysfunction is required for motor coordination to emerge. Finally, we observed a reduction in Purkinje cell innervation onto target neurons in the deep cerebellar nuclei (DCN) in $Sacs^{-/-}$ mice. Together, these findings suggest that multiple alterations in the cerebellar circuit including Purkinje cell input and output contribute to cerebellar-related disease onset in ARSACS.

Corresponding authors A. J. Watt: Department of Biology, 3649 Sir William Osler, Bellini 265, McGill University, Montreal, Quebec H3G 0B1, Canada.   Email: alanna.watt@mcgill.ca
R. A. McKinney: Department of Pharmacology and Therapeutics, 3649 Prom. Sir William Osler, Bellini 167, McGill University, Montreal, Quebec, H3G 0B1.

Introduction

Autosomal recessive spastic ataxia of Charlevoix–Saguenay (ARSACS) is an early-onset neurodegenerative disease that is estimated to be the second most common form of recessive ataxia globally (Synofzik *et al.* 2013; Thiffault *et al.* 2013). Clinical symptoms can vary across patients, but typical disease symptoms involve progressive ataxia, spasticity, speech difficulties and neuropathy (Bouchard *et al.* 1978), perhaps due to the number of different mutations that can give rise to ARSACS (Ouyang *et al.* 2006; Synofzik *et al.* 2013; Thiffault *et al.* 2013).

ARSACS is caused by inheriting two mutated copies of the *SACS* gene; although several different mutations have been identified, most are thought to produce loss-of-function early truncations of the encoded sacsin protein (Engert *et al.* 2000; Thiffault *et al.* 2013). Sacsin is a large protein (530 kDa) with multiple proposed functions, including roles in protein chaperoning (Li *et al.* 2015; Duncan *et al.* 2017), the ubiquitin–proteasome system (Parfitt *et al.* 2009) and mitochondrial function (Girard *et al.* 2012). It is expressed in several large cell types in the nervous system (Parfitt *et al.* 2009; Girard *et al.* 2012; Lariviere *et al.* 2015), including cerebellar Purkinje cells. The precise mechanism(s) giving rise to disease pathology in ARSACS are not yet fully understood, although Purkinje cell abnormalities are thought to contribute to cerebellar-related ataxia.

Both human brain imaging and post-mortem studies reveal that a common feature of ARSACS is cerebellar atrophy of the anterior cerebellar vermis, with accompanying Purkinje cell death (Bouchard *et al.* 1998; Martin *et al.* 2007). A knock-out *Sacs* mouse ($Sacs^{-/-}$) has recently been generated that displays early motor coordination abnormalities reminiscent of ataxia as well as Purkinje cell death in anterior lobules of the vermis (Lariviere *et al.* 2015), thereby recapitulating symptoms of human patients. Interestingly, Purkinje cell loss was only detected at postnatal day (P)90, well after motor coordination deficits were observed (at P40) (Lariviere *et al.* 2015). This suggests that Purkinje cell loss does not underlie early ataxia observed in ARSACS; rather, other alterations in Purkinje cells may contribute to early symptoms.

What Purkinje cell pathophysiology might contribute to early ataxia in ARSACS prior to Purkinje cell loss? Purkinje cells are the principal output neurons of the cerebellar cortical microcircuit and thus function as a linchpin in cerebellar function. They integrate massive excitatory synaptic input, as well as firing high-frequency and highly regular action potentials (ranging from ~20 to 200 Hz) in the absence of synaptic drive. Interestingly, both the excitatory input and the action potential output are altered in mouse models of several other forms of ataxia. For instance, reduced excitatory synaptic input has been reported for spinocerebellar ataxia type 1 (SCA1) (Hourez *et al.* 2011) and SCA6 (Mark *et al.* 2015), while changes in firing rate, spike precision, or both have been reported for episodic ataxia type 2 (EA2) (Walter *et al.* 2006; Alviña & Khodakhah, 2010*a,b*; Mark *et al.* 2011), SCA1 (Inoue *et al.* 2001; Hourez *et al.* 2011; Dell'Orco *et al.* 2015), SCA2 (Kasumu *et al.* 2012; Hansen *et al.* 2013; Scoles *et al.* 2017), SCA3 (Shakkottai *et al.* 2011), SCA6 (Mark *et al.* 2015; Jayabal *et al.* 2016) and SCA27 (Shakkottai *et al.* 2009). These results demonstrate that abnormalities in the input and/or output of Purkinje cells are common pathophysiological changes underlying multiple forms of ataxia arising from diverse genetic causes, leading us to wonder whether similar changes occur in ARSACS.

To address whether changes in Purkinje cell excitatory synaptic input and/or firing output contribute to early stages of ARSACS, we studied these properties in Purkinje cells from $Sacs^{-/-}$ mice. We found that excitatory synaptic drive onto $Sacs^{-/-}$ Purkinje cells was reduced, and that Purkinje cell firing rate, but not regularity, was reduced at an age when disease manifestations were first present. Firing deficits were limited to anterior lobules, and firing rates were normal in posterior lobules, which we have previously shown to not undergo cell death at later ages (Lariviere *et al.* 2015). Mild firing deficits were observed as early as P20 (prior to detectable motor deficits), suggesting that a critical level of cerebellar circuit dysfunction is

required before cerebellar-related motor coordination deficits are observed. Finally, we also observed changes in the Purkinje cell output onto their target neurons in the deep cerebellar nuclei (DCN): the number of Purkinje cell puncta apposed to large DCN neurons was reduced at P40. Together, these findings suggest that multiple alterations in the cerebellar circuit including altered Purkinje cell input and output are likely to contribute to cerebellar-related disease onset in ARSACS.

Methods

Ethical approval

Breeding and animal procedures were approved by the McGill University Animal Care Committee and were in accordance with the rules and regulations established by the Canadian Council on Animal Care.

Animals

$Sacs^{-/-}$ mice carrying a deletion of the $Sacs$ gene were generated as previously described by NorCOMM (www.norcomm.org) (Girard $et\ al.$ 2012; Lariviere $et\ al.$ 2015). Experiments were performed in litter-matched homozygous $Sacs^{-/-}$ and wild-type (WT) mice using heterozygous $Sacs^{+/-}$ breeders to control for background stain. Mice had $ad\ libitum$ access to food and water.

Acute slice preparation

Acute cerebellar slices were prepared as previously described (Watt $et\ al.$ 2009). Mice were deeply anaesthetized with isofluorane, rapidly sacrificed, and their brains were removed into ice-cold low-Ca^{2+} artificial cerebrospinal fluid (ACSF). For miniature excitatory post-synaptic current (mEPSC) experiments, ACSF contained (in mM): NaCl, 137; KCl, 2.7; $MgCl_2$, 3.5; NaH_2PO_4, 0.4; $NaHCO_3$, 11.6; $CaCl_2$, 0.5; dextrose, 5.6, with a final osmolality of ~320 mOsm and pH 7.4. For extracellular and intracellular experiments recording action potentials, ACSF contained (in mM): NaCl, 125; KCl, 2.5; $MgCl_2$, 4; NaH_2PO_4, 1.25; KCl, 2.5; $MgCl_2$, 4; NaH_2PO_4, 1.25; $NaHCO_3$, 26; $CaCl_2$, 2; dextrose, 25; with a final osmolality of ~320 mOsm and pH 7.4. The ACSF was bubbled with an O_2–CO_2 mixture (95%–5%) and acute sagittal slices (250 μm) were cut from cerebellar vermis as previously described (Watt $et\ al.$ 2009; Jayabal $et\ al.$ 2016, 2017) using a VT1200S microtome (Leica Microsystems, Wetzlar, Germany). Slices were then transferred to ACSF containing 2 mM $MgCl_2$ and 2.5 mM $CaCl_2$ for mEPSC experiments, or 1 mM $MgCl_2$ and 2 mM $CaCl_2$ for action potential recordings. Slices were incubated for 30−45 min at 37°C and then removed to room temperature, where they were stored in continuously bubbling ACSF for up to an additional 8 h.

Electrophysiology

For whole-cell mEPSC experiments, an internal solution was used containing (in mM): 120 potassium gluconate, 1 EGTA, 10 HEPES, 5 Mg-ATP, 0.5 Na-GTP, 5 NaCl, 5 KCl, 10 phosphocreatine, with 295 mOsm and pH 7.3 (adjusted with KOH). Patch-pipettes of 5−7 MΩ were used for both patch and extracellular/loose patch recordings. For whole-cell mEPSC recordings, gigaohm seals were obtained and Purkinje cells from P40 mice were voltage-clamped to −60 mV at room temperature as previously described (Chang $et\ al.$ 2014, 2015). AMPA-mediated mEPSC were isolated using 1 μM tetrodotoxin, 15 μM 3-[(R)-2-carboxypiperazin-4-yl]-propyl-1-phosphonic acid (CPP), 100 μM picrotoxin and 1 μM CGP55845 in the ACSF. Analysis was performed offline using miniAnalysis (Synaptosoft, Decatur, GA, USA) and/or Igor Pro (Wavemetrics, Portland, OR, USA). Average mEPSCs were used to calculate the 10–90% rise time, and the τ_{decay} time constant was measured by fitting a single exponential.

Spontaneous Purkinje cell firing was non-invasively recorded at 33.5−34.5°C using extracellular/loose patch recording with electrodes pulled with a P-1000 puller (Sutter Instruments, Novato, CA, USA) filled with ACSF. Recordings were made either with or without fast synaptic blockade: fast synaptic currents were blocked during spontaneous recordings with 10 μM 6,7-dinitroquinoxaline-2,3-dione (DNQX), 50 μM 2-amino-5-phosphonopentanoate (AP-V) and 10 μM SR95531 (GABAzine). Spike times were analysed using custom routines in Igor Pro 6.0. Anterior lobule recordings were made in Lobule III, and posterior lobule recordings were made in Lobule IX.

For action potential whole-cell current-clamp recordings, patch pipettes (3−5 MΩ) were filled with internal solution (100 mM potassium gluconate, 10 mM HEPES, 20 mM KCl, 2 mM Na2ATP, 2 mM MgATP, 0.4 mM Na_2GTP, 0.05 mM EGTA, 0.2% biocytin; pH 7.3) and synaptic blockers (10 μM SR-95531, 10 μM DNQX, 50 μM APV) were added to the ACSF. Automatic pipette capacitance compensation from a Multiclamp 700B amplifier (Molecular Devices, Sunnyvale, CA, USA) was used during all recordings. After hyperpolarization (AHP) was measured as the minimum negative peak found after the action potential. Maximum instantaneous frequency was calculated as the maximum firing frequency between two consecutive spikes at the highest current injection. All chemicals were purchased from Sigma-Aldrich (Oakville, ON, Canada) unless noted otherwise.

Immunocytochemistry

Mice were deeply anaesthesized with avertin (2,2,2-tribromolethanol; 250 mg kg^{-1}) administered via intraperitoneal injection, and subsequently a trans-cardial perfusion of phosphate-buffered saline (PBS; pH 7.4 with 200 ml ml^{-1} heparin) followed by 2% paraformaldehyde was performed to preserve brain structure. To compare the sizes of the fastigial and interposed nuclei, coronal slices were prepared from WT and *Sacs*$^{-/-}$ mice, and DCN neurons were labelled with anti-NeuN, shown in yellow pseudo-colour. The nuclei were identified from comparable locations in the cerebellum in WT and *Sacs*$^{-/-}$ mice, outlined, and their area calculated in ImageJ. To label Purkinje cell positive puncta in the DCN, rabbit anti-calbindin antibody was used in combination with an Alexa-594-conjugated anti-rabbit secondary antibody. A minimum of 10 sagittal slices per animal were collected at spaced intervals throughout the vermis to ensure that we sampled across the tissue. DCN neurons were labelled with Alexa488-tagged anti-NeuN (Millipore, Etobicoke, ON, Canada). Two-photon image stacks were acquired at 830 nm (red channel) and 775 nm (green channel) with 1024 × 1024 resolution on a custom two-photon microscope. The density of DCN neurons was measured using binary images of DCN nuclei and a custom-written script in ImageJ. The number of cells was verified using a composite image. DCN cell numbers are reported as number of cells/100 μm^2. Purkinje cell synapses onto DCN cells were analysed by counting the number of puncta surrounding large DCN cells (>15 μm diameter). In a separate set of experiments, we used anti-rat vesicular GABA transporter antibody (VGAT: Cedarlane, Burlington, ON, Canada) and rabbit anti-calbindin, and the number of VGAT$^+$ puncta on large DCN cells that co-labelled for calbindin was used to calculate the percentage of inhibitory puncta that arise from Purkinje cells. All imaging was acquired and analysed blind to condition, and images are presented in pseudocolour.

Behaviour

P20 WT and *Sacs*$^{-/-}$ animals were tested in two behavioural assays. For a rotarod assay, animals were placed on a rotarod apparatus (Stoelting Europe, Dublin, Ireland) using a 10 min-long accelerating assay as previously described (Jayabal *et al.* 2015). Mice performed four trials per day over four consecutive days of testing. The latency to fall was recorded for each trial. The data are presented as the day average of the four trials for each day and condition. For an elevated beam assay, animals were made to walk along raised round wooden beams of 10 and 8 mm diameter (100 cm long) towards a dark escape box. Mice were first trained for one day using a 12 mm round beam followed by two days of testing. During each testing day mice performed three trials on each beam, and we recorded the time taken to traverse 80 cm on the beams. The results shown are the average of the two best trials for each testing day.

Statistics

Comparisons were made using Student's paired or unpaired *t* test for normally distributed data or the Mann–Whitney *U* test when data were not normally distributed using Igor Pro or JMP (SAS Institute, Cary, NC, USA) software. Data are typically represented as mean ± SEM, and in some cases, histograms are also shown. Unless otherwise indicated, *N* is the number of animals, and *n* is the number of cells.

Results

Altered glutamatergic input to cerebellar Purkinje cells in ARSACS mice

Purkinje cells receive glutamatergic input from two major inputs: one strong climbing fibre synapse that makes multiple synaptic contacts with the Purkinje cell, and parallel fibres, with one Purkinje cell receiving input from >150,000 parallel fibres (Napper & Harvey, 1988). Since altered glutamatergic synaptic transmission has been implicated in mouse models of other forms of ataxia (Hourez *et al.* 2011; Mark *et al.* 2015), we wondered whether there were changes in glutamatergic transmission in *Sacs*$^{-/-}$ mice that might contribute to disease onset.

Motor coordination deficits have been reported as early as P40 in *Sacs*$^{-/-}$ mice (Lariviere *et al.* 2015), so we used P50–60 mice to examine glutamatergic synaptic transmission after the onset of motor phenotype. We performed whole-cell recordings from Purkinje cells in acute slices of *Sacs*$^{-/-}$ and WT control mice, and measured mEPSCs (Fig. 1*A* and *B*). In contrast to what has been observed in other ataxias (e.g. Hourez *et al.* 2011), we found that mEPSC amplitude was enhanced in *Sacs*$^{-/-}$ compared to WT Purkinje cells (WT mEPSC amplitude = 10.4 ± 0.4 pA, *N* = 3 mice, *n* = 16 cells; *Sacs*$^{-/-}$ mEPSC amplitude = 12.0 ± 0.4 pA, *N* = 4, *n* = 11; *P* = 0.038; Fig. 1*B* and *C*). Contrary to this enhancement in mEPSC amplitude in *Sacs*$^{-/-}$ Purkinje cells, however, we observed a reduction in mEPSC frequency, as shown by an increased mEPSC inter-event interval (IEI) (WT IEI = 376.7 ± 29.8 ms; *Sacs*$^{-/-}$ IEI = 456.0 ± 64.2 ms; *P* = 0.043; Fig. 1*D*). These results suggest that either a presynaptic reduction in release probability or an increase in the number of silent synapses, in addition to post-synaptic enrichment of receptors likely contributes to changes in glutamatergic transmission onto Purkinje cells

in $Sacs^{-/-}$ mice. To disentangle whether changes arose pre- or postsynaptically, we further analysed mEPSC kinetics by measuring the rise time and decay time constant (τ_{decay}). We found no significant differences in the rise time (WT: 5.1 ± 0.26 ms; $Sacs^{-/-}$: 5.6 ± 0.48 ms, $P = 0.35$; Fig. 1E), suggesting that we were sampling populations of synapses that were located at similar distances from the soma in both genotypes (Sjostrom & Hausser, 2006). We also found no significant differences in τ_{decay} in $Sacs^{-/-}$ and WT Purkinje cells (WT: 3.4 ± 0.26 ms; $Sacs^{-/-}$: 4.1 ± 0.64 ms; $P = 0.26$; Fig. 1F), suggesting that subunit composition at these excitatory synapses is unchanged in $Sacs^{-/-}$ mice (Lalanne et al. 2016).
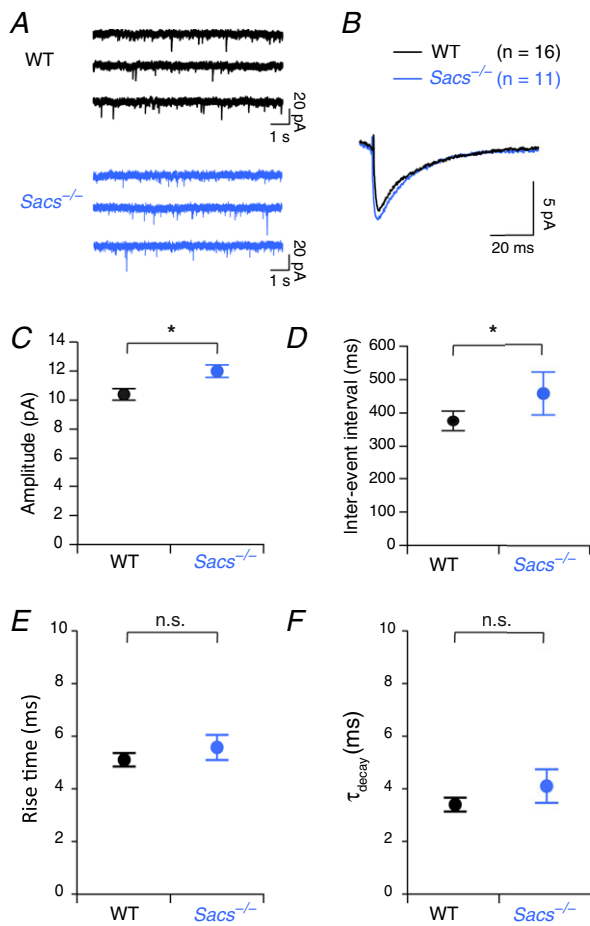
Figure 1. Altered glutamatergic input to Purkinje cells in P60 $Sacs^{-/-}$ mice

A, sample traces of AMPA-mediated miniature current recordings from representative WT (top, black) and $Sacs^{-/-}$ Purkinje cells (bottom, blue). B, superimposed average traces of AMPA-mediated mEPSCs from WT and $Sacs^{-/-}$ Purkinje cells. C, an increase of average mEPSC amplitude is observed. D, this is accompanied by an increase of the inter-event interval in $Sacs^{-/-}$ Purkinje cells in comparison to WT. E and F, neither the rise time (E) nor the decay time constant (τ_{decay}; F) is significantly different in WT or $Sacs^{-/-}$ Purkinje cells. WT: $N = 3$, $n = 16$; $Sacs^{-/-}$: $N = 4$, $n = 11$. n.s., $P > 0.05$; *$P < 0.05$.

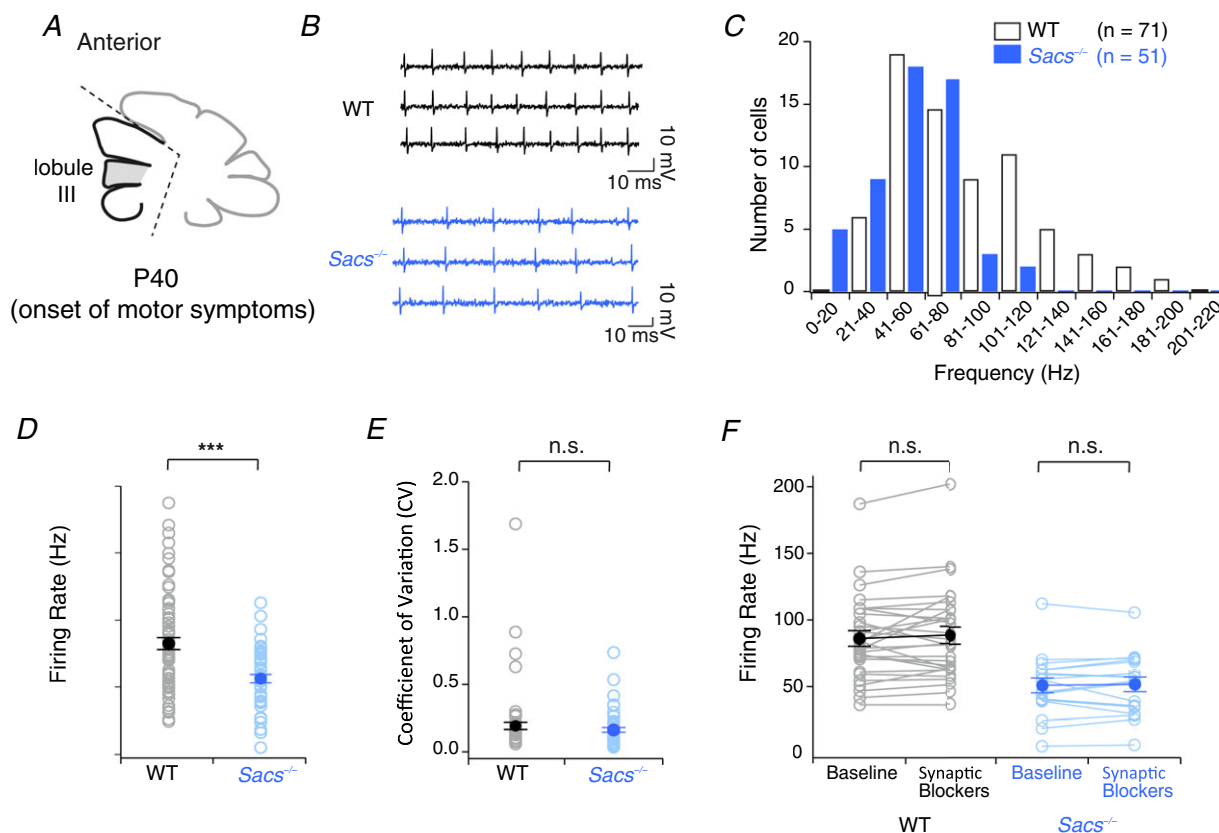## Lobule-specific changes in Purkinje cell firing

Next, we wanted to examine whether changes in Purkinje cell spiking output were observed in $Sacs^{-/-}$ mice that display early motor coordination deficits, since changes in firing properties have been observed in several other forms of ataxia when motor symptoms are present (e.g. Walter et al. 2006; Hourez et al. 2011; Shakkottai et al. 2011; Jayabal et al. 2016). Since Purkinje cell death occurs predominantly in anterior lobules, we restricted our recordings to anterior lobule III (Fig. 2A). We performed cell-adjacent loose-patch or extracellular recordings from visually identified Purkinje cells to non-invasively measure their firing properties (Fig. 2B). We found that individual WT Purkinje cells fired action potentials at a set, characteristic frequency that ranged from ∼20 to 200 Hz (Fig. 2C), with an average firing frequency of 82.5 ± 4.4 Hz ($N = 11$ mice, $n = 71$ cells) (Fig. 2D). The firing rates of $Sacs^{-/-}$ Purkinje cells were lower, covering a narrower range of frequencies (from 10 to 120 Hz; Fig. 2C), and showing a significantly reduced average frequency (56.4 ± 3.1 Hz, $N = 9$, $n = 51$; $P = 0.0002$; Fig. 2D). Although firing frequency was reduced, there was no significant difference in the regularity of firing, since the coefficient of variation (CV) of interspike intervals in $Sacs^{-/-}$ was unchanged from WT Purkinje cells (WT: $CV = 0.21 \pm 0.18$; $Sacs^{-/-}$: $CV = 0.14 \pm 0.08$; $P = 0.21$; Fig. 2E).

To determine whether changes in spontaneous Purkinje cell firing arose from alterations in fast synaptic transmission, as has been previously reported (Häusser & Clark, 1997), we recorded spontaneous action potentials from Purkinje cells before and after applying a cocktail of synaptic blockers of fast excitatory and inhibitory neurotransmission. Synaptic blockade did not affect spontaneous spike frequency in WT or $Sacs^{-/-}$ Purkinje cells (WT: without drug average firing: 86.1 ± 5.9 Hz; after drug cocktail: 88.9 ± 6.5 Hz, $N = 7$, $n = 29$, $P = 0.29$; $Sacs^{-/-}$: without drug average firing: 50.6 ± 3.1 Hz; after drug cocktail: 51.4 ± 3.2 Hz, $N = 6$, $n = 19$, $P = 0.55$; Fig. 2F). Thus, although changes in fast glutamatergic synaptic transmission are observed in $Sacs^{-/-}$ Purkinje cells (Fig. 1), they do not contribute to the changes in spontaneous firing properties we observe in acute slice recordings (Fig. 2F), likely because excitatory inputs are largely silent in acute slices.

Do changes observed in Purkinje cell firing arise at the same time as motor coordination deficits? To determine whether alterations in Purkinje cell firing properties preceded motor coordination deficits we recorded from anterior lobule Purkinje cells from younger mice (P20; Fig. 3A). We found that as early as P20, high-frequency firing rates were observed in WT Purkinje cells (average P20 WT frequency = 84.2 ± 3.2 Hz, $N = 3$, $n = 31$; Fig. 3B), although the frequency range of recorded neurons was narrower than in older mice (compare Figs 3B and

2*C*) because firing properties are not fully mature at P20 (McKay & Turner, 2005; Watt *et al.* 2009; Arancillo *et al.* 2015). We also observed a small but significant reduction in the range and average firing rate in *Sacs*$^{-/-}$ Purkinje cells at P20 (average P20 *Sacs*$^{-/-}$ frequency = 73.5 ± 4.1 Hz, $N = 5$, $n = 38$; $P = 0.0026$; Fig. 3*B* and *C*). In agreement with our observations at P40, we observed no significant changes in the regularity of firing (WT P20 CV = 0.18 ± 0.01; *Sacs*$^{-/-}$ P20 CV = 0.16 ± 0.01; $P = 0.05$; Fig. 3*D*). Impaired motor coordination has been observed in *Sacs*$^{-/-}$ mice as early as P40 (Lariviere *et al.* 2015), but has not been tested at earlier ages. However, ARSACS is an early-onset disease that can be detected in infants in humans (Synofzik *et al.* 2013), which suggests that early motor impairment may be observed in *Sacs*$^{-/-}$ mice as well. To test this, we performed rotarod and elevated beam assays, which are often used to characterize ataxia in mouse models (Jayabal *et al.* 2015). No significant differences were observed in *Sacs*$^{-/-}$ mice in either

rotarod performance (Day 4 rotarod time on beam: WT: 82.4 ± 6.4 s, $N = 9$; *Sacs*$^{-/-}$: 96.4 ± 12.1 s, $N = 8$; $P = 0.17$; Fig. 3*E*) or in elevated beam (Day 2 latency to cross the beam: WT: 6.3 ± 1.4 s; *Sacs*$^{-/-}$: 8.7 ± 2.2 s; $P = 0.37$; Fig. 3*F*). This suggests that significant motor coordination impairment is not detectable in *Sacs*$^{-/-}$ mice until the end of postnatal development (Lariviere *et al.* 2015), although it is possible that subtle changes in motor performance occur earlier but cannot be detected through these assays. Given that the magnitude of firing frequency reduction in *Sacs*$^{-/-}$ mice at P20 (~15 %) was smaller than that at P40 (~45 %), our data suggest that a critical level of impairment is required for motor abnormalities to become detectable with these assays. However, other early changes have been observed in Purkinje cells, such as aberrant neurofilament accumulation in dendrites at P14 (Lariviere *et al.* 2015), arguing that motor dysfunction may arise from an expanding constellation of alterations that impair cellular function.
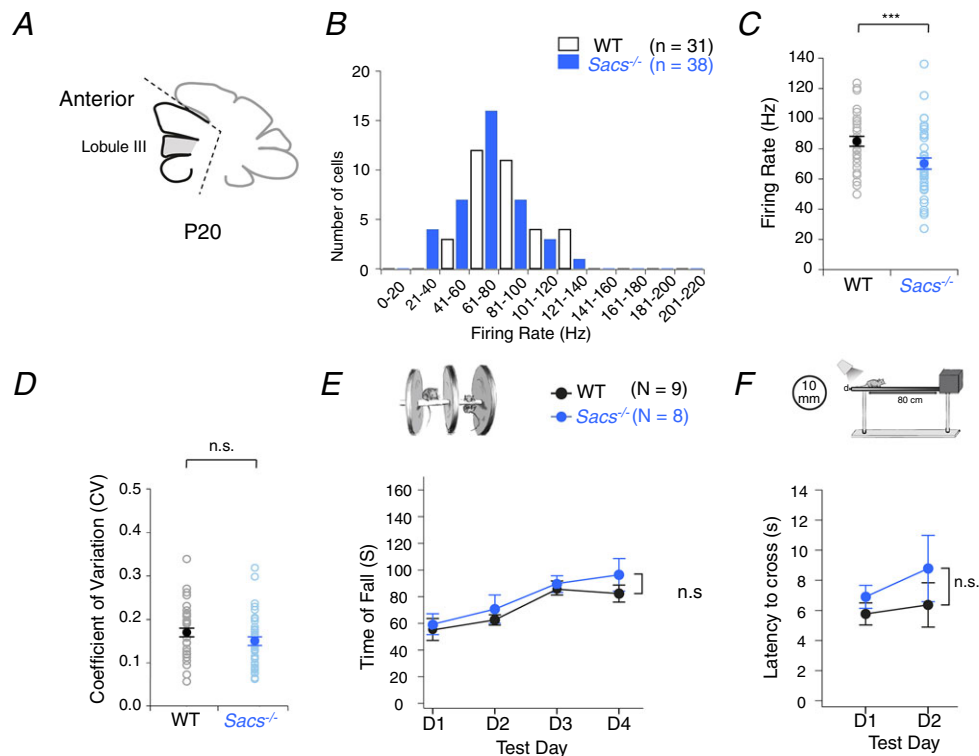

Figure 2. Reduced firing rate of anterior Purkinje cells in P40 *Sacs*$^{-/-}$ mice
A, schematic representation showing anterior lobule recording site (in grey) and animal age. *B*, sample spike trains from representative WT (top, black) and *Sacs*$^{-/-}$ (bottom, blue) Purkinje cells from anterior lobule III. *C*, frequency histogram of Purkinje cell firing is shifted left in *Sacs*$^{-/-}$ mice compared to WT, with no high-frequency Purkinje cells present in *Sacs*$^{-/-}$ cerebellum. *D*, firing rate in *Sacs*$^{-/-}$ Purkinje cells is significantly lower than WT. *E*, however, no changes in the coefficient of variation (CV) of interspike intervals is observed in *Sacs*$^{-/-}$ mice. *F*, acute blockade of fast excitatory and inhibitory synaptic inputs onto Purkinje cells (Synaptic blockers) did not significantly affect spontaneous firing in WT or *Sacs*$^{-/-}$ mice ($P > 0.05$). WT: $N = 11$, $n = 71$; *Sacs*$^{-/-}$: $N = 9$, $n = 51$ for *A–E*; WT: $N = 7$, $n = 29$; *Sacs*$^{-/-}$: $N = 6$, $n = 19$ for *F*. n.s., $P > 0.05$; ***$P < 0.001$.

To gain further insight on the mechanistic underpinnings of the observed reduction in firing rates in anterior lobule $Sacs^{-/-}$ Purkinje cells at P40 (Fig. 4A), we made whole-cell recordings from Purkinje cells from WT and $Sacs^{-/-}$ mice (Fig. 4B). We measured several properties of action potentials, since changes in intrinsic Na^+ and K^+ conductance typically result in alterations in spike shape. We measured the amplitude and half-width of action potentials, as well as the magnitude of AHP that follows (Fig. 4C). Interestingly, we found that there were no significant differences between these properties in $Sacs^{-/-}$ Purkinje cells compared to WT ($N = 5$, $n = 10$ WT; $N = 6$, $n = 10$ for $Sacs^{-/-}$; $P = 0.23$ for spike height; $P = 0.36$ for half-width; $P = 0.11$ for AHP; Fig. 4D–F), suggesting that the fast conductances contributing to action potentials are not altered in $Sacs^{-/-}$ Purkinje cells. This contrasts with what has been observed in mouse models of other forms of ataxia (e.g. Inoue $et\ al.$ 2001; Walter $et\ al.$ 2006).

Changes in spike shape might be expected if there were alterations in the properties of K^+ channels. Nonetheless, we tested whether low concentrations of the broad-spectrum K^+ blocker 4-aminopyridine (4-AP) would alter spiking, since this has been shown to reverse firing deficits in mouse models of other forms of ataxia (Alviña & Khodakhah, 2010b; Hourez $et\ al.$ 2011; Jayabal $et\ al.$ 2016) demonstrating therapeutic potential. However, we found that acute administration of 4-AP at low concentrations (5 and 10 μM) that affected firing in other ataxia models (e.g. Alviña & Khodakhah, 2010b) did not alter the firing rates of anterior lobule $Sacs^{-/-}$ Purkinje cells (for 5 μM 4-AP: WT frequency before drug = 62.1 ± 3.0 Hz, frequency after 5 μM 4-AP = 60.8 ± 8.2 Hz, $N = 2$, $n = 6$, not significantly different, paired t test, $P = 0.86$; $Sacs^{-/-}$ frequency before drug = 42.9 ± 2.8 Hz, frequency after 5 μM 4-AP = 46.4 ± 2.6 Hz, $N = 2$, $n = 8$, $P = 0.38$; for 10 μM 4-AP: WT frequency before drug = 55.6 ± 9.3 Hz, frequency after 10 μM 4-AP = 59.4 ± 9.3 Hz, $N = 4$, $n = 9$, $P = 0.39$; $Sacs^{-/-}$ frequency before drug = 38.5 ± 2.7 Hz, frequency after 10 μM 4-AP = 43.2 ± 5.9 Hz, $N = 5$, $n = 15$, $P = 0.28$; Fig. 5). This suggests that 4-AP is not likely to show therapeutic benefits in $Sacs^{-/-}$ mice or indeed in ARSACS.

To better understand the changes underlying the reduction in intrinsic excitability in anterior-lobule

**Figure 3. Reduced firing rate of P20 anterior $Sacs^{-/-}$ Purkinje cells precedes ataxia onset**
A, schematic representation showing recordings made from anterior lobules at P20 (in grey). B, histogram showing distribution of firing rates is similar in WT (open bars) and $Sacs^{-/-}$ (blue) Purkinje cells. C and D, nonetheless, there is a small reduction in the average firing rate of $Sacs^{-/-}$ Purkinje cells (C) without a change in the CV of interspike interval (D). E and F, motor coordination defects evaluated by rotarod assays (E) and the latency to cross a balance beam (F) are not yet detectable in $Sacs^{-/-}$ mice. WT: $N = 3$, $n = 31$; $Sacs^{-/-}$: $N = 5$, $n = 38$ for A–D; WT: $N = 8$; $Sacs^{-/-}$: $N = 8$ for E and F. n.s., $P > 0.05$; ***$P < 0.005$.
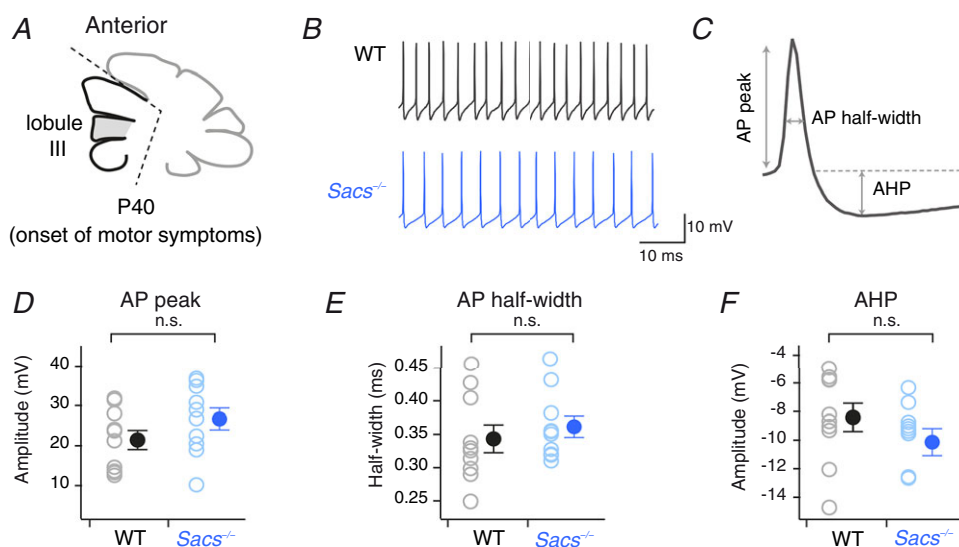
Figure 4. Action potential waveforms are not different in *Sacs*⁻ᐟ⁻ Purkinje cells
A, schematic representation showing anterior lobule recording site (in grey) and animal age. *B*, sample intracellular action potential waveforms recorded from WT (top, black) and *Sacs*⁻ᐟ⁻ (bottom, blue) Purkinje cells from anterior lobules. *C*, sample action potential from WT Purkinje cell showing spike property measurements action potential (AP) peak and half-width, as well as after-hyperpolarization (AHP) amplitude. *D–F*, AP peak (*D*), half-width (*E*) and AHP amplitude (*F*) are not significantly different for spikes measured from *Sacs*⁻ᐟ⁻ Purkinje cells and WT. WT: $N = 5$, $n = 10$; *Sacs*⁻ᐟ⁻: $N = 6$, $n = 10$. n.s., $P > 0.05$.

Sacs⁻ᐟ⁻ Purkinje cells (Fig. 6*A*), we performed whole-cell recordings and injected current steps to elicit changes in action potential firing frequency (Fig. 6*B*) to construct input−output curves for WT and *Sacs*⁻ᐟ⁻ Purkinje cells (Fig. 6*C*). We found that at high current injection amplitudes, *Sacs*⁻ᐟ⁻ Purkinje cells fired at significantly reduced frequencies compared to WT Purkinje cells
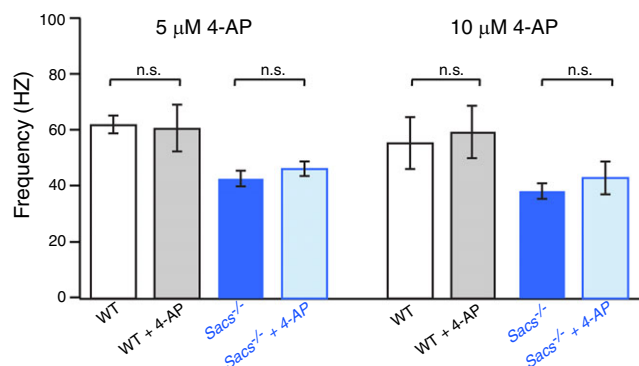
Figure 5. 4-AP does not affect firing properties in *Sacs*⁻ᐟ⁻ mice
We acutely applied 5 μM (left) and 10 μM (right) 4-AP to WT (before: open bar; after: grey) and *Sacs*⁻ᐟ⁻ mice (before: bright blue; after: light blue), and found no significant changes in frequency for either WT or *Sacs*⁻ᐟ⁻ Purkinje cells (5 μM: $N = 2$, $n = 6$ WT; $N = 2$, $n = 8$ *Sacs*⁻ᐟ⁻ Purkinje cells; 10 μM: $N = 4$, $n = 9$ WT; $N = 5$, $n = 15$ *Sacs*⁻ᐟ⁻ Purkinje cells). These concentrations of 4-AP have been shown to affect Purkinje cell firing rate in other mouse models of ataxia, likely through the action of K_v1 type channels (Alviña & Khodakhah, 2010*b*). n.s., $P > 0.05$.

($N = 8$, $n = 10$ for WT; $N = 8$, $n = 13$ for *Sacs*⁻ᐟ⁻ up to 0.1 nA current injection; $N = 3$, $n = 5$ for WT; $N = 4$, $n = 8$ for *Sacs*⁻ᐟ⁻ for all other current injections; *Sacs*⁻ᐟ⁻ is significantly different from WT for injections ≥0.08 nA; Fig. 6*C*). In agreement with this, the maximum firing frequency for a given current injection (0.24 nA) was reduced in *Sacs*⁻ᐟ⁻ Purkinje cells compared to WT (WT max. frequency = 276.8 ± 24.7 Hz, $N = 3$, $n = 5$; *Sacs*⁻ᐟ⁻ max. frequency = 188.4 ± 17.2 Hz, $N = 4$, $n = 8$; significantly different, $P = 0.02$; Fig. 6*D*). However, there was no significant difference observed in the maximum instantaneous firing frequency (WT max. instantaneous frequency = 348.0 ± 19.4 Hz; *Sacs*⁻ᐟ⁻ max. instantaneous frequency = 312.1 ± 11.9 Hz; not significantly different, $P = 0.14$; Fig. 6*E*), meaning that *Sacs*⁻ᐟ⁻ Purkinje cells have the capacity to fire briefly at high frequencies, just not for a sustained duration. This supports our earlier interpretation of our findings that a lack of change in the shape of action potentials in *Sacs*⁻ᐟ⁻ Purkinje cells reflects normal expression of fast voltage-dependent Na⁺ and K⁺ conductances. These results suggest that reduced Purkinje cell firing frequency in *Sacs*⁻ᐟ⁻ mice may be linked to their inability to sustain high-frequency firing (e.g. compare top WT and *Sacs*⁻ᐟ⁻ traces in Fig. 6*B*, *D* and *E*).

Since Purkinje cell loss occurs predominantly in anterior lobules in *Sacs*⁻ᐟ⁻ mice (Lariviere *et al.* 2015), we focused on anterior lobule III when recording firing rates. However, we wondered whether these changes that we observed in firing in anterior lobules (Figs 3, 4 and 6) are widespread. To address this question, we recorded

spontaneous Purkinje cell firing from posterior lobule IX at the age when motor symptoms are detectable (P40; Fig. 7A). We found that WT Purkinje cells fired action potentials with a smaller and lower range of frequencies than in anterior lobules (0–140 Hz; average frequency 51.1 ± 3.1 Hz, $N = 5$, $n = 56$; Fig. 7B and C), as previously described (Kim *et al.* 2012). Interestingly, firing rates in $Sacs^{-/-}$ Purkinje cells from posterior lobules did not differ from WT (average frequency 47.8 ± 2.5 Hz, $N = 8$, $n = 59$; $P = 0.42$; Fig. 7B and C). Furthermore, WT firing was observed to be regular in posterior lobules, which was also unaltered in $Sacs^{-/-}$ Purkinje cells (WT: CV = 0.10 ± 0.01; $Sacs^{-/-}$: CV = 0.09 ± 0.01; $P = 0.08$; Fig. 7D). These data support the hypothesis that Purkinje cell firing deficits are linked to later Purkinje cell death since firing alterations are only seen in lobules that later undergo degeneration.

Circuit alterations in the deep cerebellar nuclei

Purkinje cell firing properties reflect the temporal output of Purkinje cells, which is transmitted along Purkinje cell axons to target neurons in the DCN. DCN neurons project to extra-cerebellar targets in the brain and spinal cord

and thus transmit information outside the cerebellum. Interestingly, accumulation of neurofilament has been observed in the DCN to a similar extent to the neurofilament accumulation in Purkinje cells in $Sacs^{-/-}$ mice (Lariviere *et al.* 2015), which suggests that DCN deficits may contribute to pathophysiology in $Sacs^{-/-}$ mice.

To confirm that calbindin-positive puncta in the DCN are likely to reflect functional GABAergic presynaptic terminals in our animals, we quantified the number of puncta that stain for a presynaptic GABA terminal marker (VGAT; Fig. 8A) that co-localizes with calbindin-positive puncta. We found that most GABAergic puncta are calbindin positive in both WT and $Sacs^{-/-}$ DCN at P40 (WT calbindin/VGAT ratio: 0.83 ± 0.02, $N = 4$, $n = 26$ cells; $Sacs^{-/-}$ calbindin/VGAT ratio: 0.81 ± 0.02, $N = 4$, $n = 33$ cells; not significantly different, $P = 0.56$; Fig. 8B) (Husson *et al.* 2014). This suggests that calbindin-positive puncta reflect functional Purkinje cell presynaptic terminals in both WT and $Sacs^{-/-}$ mice.

To address whether alterations in DCN are observed in $Sacs^{-/-}$ mice, we used immunocytochemistry to identify and quantify the DCN at P40, when motor deficits are first
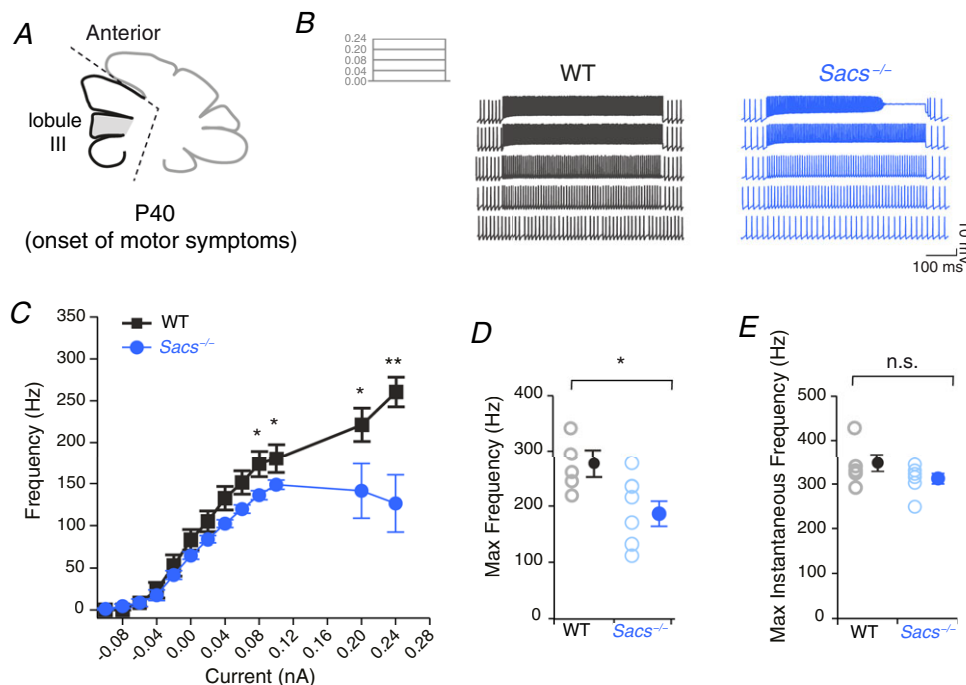

Figure 6. Changes in the input–output function of $Sacs^{-/-}$ Purkinje cells reflect inability to sustain high-frequency firing
A, schematic representation showing anterior lobule recording site (in grey) and animal age. *B*, sample traces from WT (black) and $Sacs^{-/-}$ (blue) Purkinje cells showing evoked action potential firing for a given current injection, as indicated in inset (left, nA). *C*, summary input–output curve data reveal that $Sacs^{-/-}$ (blue) Purkinje cells show reduced firing frequency with higher current injection amplitudes compared to WT (black). *D*, in agreement, the highest frequency firing each cell achieves is reduced in $Sacs^{-/-}$ Purkinje cells compared to WT (frequency measured for 0.24 pA current injection). *E*, however, the maximum instantaneous firing rate is not altered. WT: $N = 8$, $n = 10$; $Sacs^{-/-}$: $N = 8$, $n = 13$ for injections up to 0.1 nA; WT: $N = 3$, $n = 5$; $Sacs^{-/-}$: $N = 4$, $n = 8$ for all other current injections, including data in *D* and *E*. n.s., $P > 0.05$; *$P < 0.05$; **$P < 0.01$.

observed. First, we examined whether changes in the gross morphology of the fastigial or interposed nuclei (FN, left; and IN, right) were observed (Fig. 9*A*), since these are the nuclei that receive projections from vermis (Voogd, 2011). We observed no significant differences in the size of either nucleus (FN: WT: $3.6 \times 10^5 \pm 0.18 \times 10^5$ μm^2, $N = 4$ mice; $Sacs^{-/-}$: $3.3 \times 10^5 \pm 0.21 \times 10^5$ μm^2, $N = 3$; $P = 0.31$; IN: WT: $4.7 \times 10^5 \pm 0.43 \times 10^5$ μm^2; $Sacs^{-/-}$: $5.1 \times 10^5 \pm 0.45 \times 10^5$ μm^2; $P = 0.51$; Fig. 9*B*). In addition, we observed no differences in the density of large DCN neurons (>15 μm diameter; De Zeeuw & Berrebi, 1995; Person & Raman, 2012; Husson *et al.* 2014) in WT and $Sacs^{-/-}$ mice (WT: 1.85 ± 0.12 cells/100 μm^2, $N = 4$ mice; $Sacs^{-/-}$: 1.81 ± 0.12 cells/100 μm^2, $N = 4$ mice; not significantly different, $P = 0.81$; Fig. 9*C* and *D*). Taken together, these results suggest that DCN degeneration does not occur in $Sacs^{-/-}$ mice at this age.

Purkinje cells make strong synapses onto DCN neurons (Person & Raman, 2012), which is reflected morphologically by the large number of Purkinje cell puncta that coat the somata of DCN neurons (Figs 8*A* and 9*E*) (Husson *et al.* 2014). To quantify the number of Purkinje cell terminals that were made onto principal projection neurons, we identified large DCN neurons in WT and $Sacs^{-/-}$ mice and counted the number of calbindin-positive puncta apposed to them (Fig. 9*E* and *F*). We found that the number of Purkinje cell calbindin positive puncta made onto individual DCN neurons was reduced in $Sacs^{-/-}$ mice compared to WT (WT: 38.0 ± 1.1 puncta per large cell; $Sacs^{-/-}$: 26.3 ± 0.82 puncta per large cell; $P < 0.00001$; Fig. 9*F*), suggesting that Purkinje cell input into neurons in the DCN is decreased in $Sacs^{-/-}$ mice. A reduction of Purkinje cell input in the DCN will likely have a profound effect on cerebellar output and function.
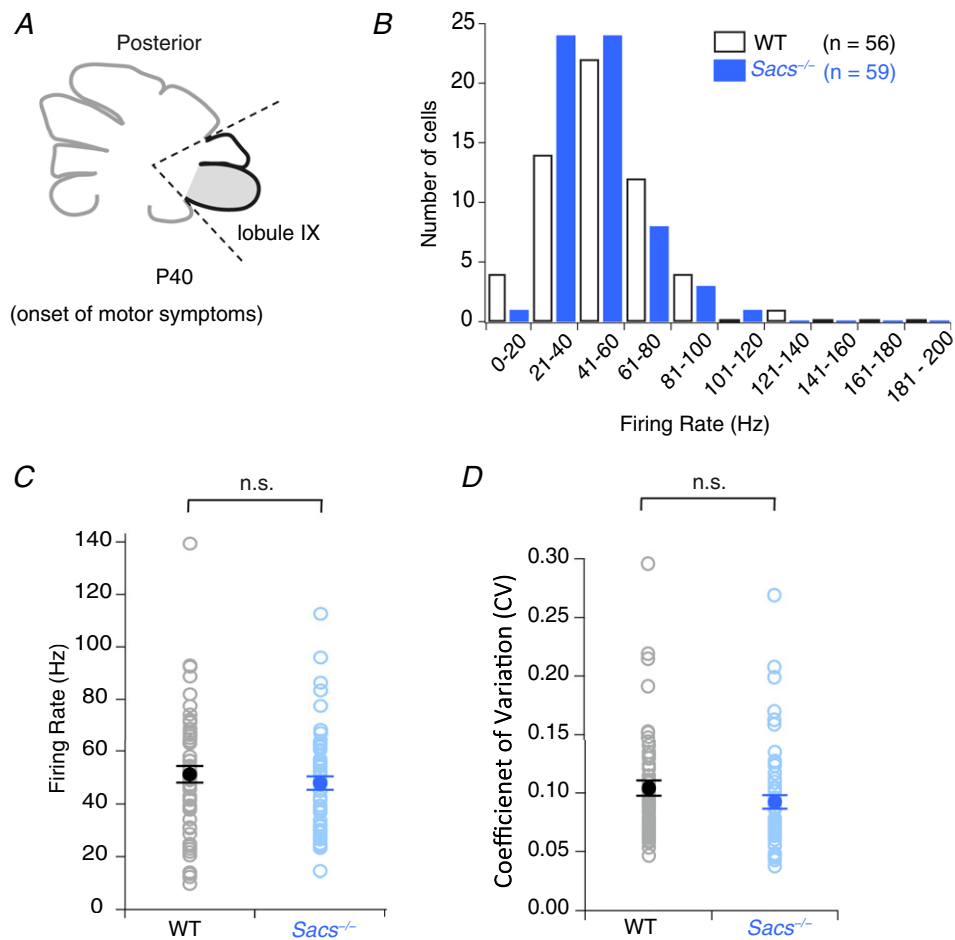
**Figure 7. Unaltered firing properties of posterior lobule Purkinje cells in P40 $Sacs^{-/-}$ mice**
A, schematic representation showing posterior lobule recording site (in grey). *B*, frequency histogram shows both WT (unfilled columns) and $Sacs^{-/-}$ (blue columns) Purkinje cells fire at frequencies below 120 Hz. *C* and *D*, average firing rate (*C*) and CV of interspike interval (*D*) are not significantly different between $Sacs^{-/-}$ and WT Purkinje cells. WT: $N = 5$, $n = 56$; $Sacs^{-/-}$: $N = 8$, $n = 59$. n.s., $P > 0.05$.

Discussion

Here we describe functional changes in Purkinje cell innervation and firing and synaptic output in a mouse model of ARSACS that may contribute to disease onset. We found a small increase in the size of synaptic inputs as well as a decrease in the frequency of miniature synaptic events, without detectable changes in postsynaptic sub-unit composition or synapse location. In addition to changes in mEPSC input, we observed a reduction in the firing frequency, but not firing regularity, of Purkinje cells. The reduction in firing frequency was due to the absence of high-firing cells that is observed in wild-type Purkinje cells in anterior lobules. This reduced firing was not due to changes in fast excitatory or inhibitory input, and was not accompanied by changes in the shape of the Purkinje cell action potentials. Although Purkinje cells could briefly maintain periods of high-frequency firing with current injections, they were unable to sustain this firing over long durations. Changes in firing likely occur gradually, with a small but significant reduction observed as early as P20, an age prior to discernible motor symptoms being detected. These changes are localized to anterior lobules that later degenerate (Lariviere *et al.* 2015). Finally, although DCN size and cell density were not affected, we observe alterations in their innervation: fewer Purkinje cell puncta innervate the somata of large projection neurons in the DCN. Together, these findings suggest that changes in both Purkinje cell input and output, as well as intrinsic changes in firing properties, may contribute to cerebellar dysfunction in ARSACS. Previously, alterations in mitochondria, neurofilament localization, and dendritic structure have been reported in this mouse model of ARSACS (Girard *et al.* 2012; Lariviere *et al.* 2015; Duncan *et al.* 2017). It will be of interest to determine how and if the functional changes we have characterized in this study relate to already described structural changes. It is likely that the accumulation of multiple different cellular abnormalities contributes to cell loss in Purkinje cells in anterior lobules in ARSACS. Which of these alterations contributes most to Purkinje cell death? Given the prevalence of synaptic and firing rate deficits observed across several ataxias and that therapeutic strategies aimed at restoring these functions were found to alleviate motor deficits (Inoue *et al.* 2001; Walter *et al.* 2006; Shakkottai *et al.* 2009, 2011; Alviña & Khodakhah, 2010*a,b*; Hourez *et al.* 2011; Mark *et al.* 2011; Kasumu *et al.* 2012; Hansen *et al.* 2013; Dell'Orco *et al.* 2015; Mark *et al.* 2015; Jayabal *et al.* 2016; Power *et al.* 2016; Shuvaev *et al.* 2017) changes in synaptic and firing properties are particularly good candidates for contributing to pathophysiology in ARSACS.

Synaptic alterations are observed in excitatory synapses made onto Purkinje cells in several animal models of ataxia. Typically, these changes reflect decreases in synaptic strength (e.g. Hourez *et al.* 2011; Mark *et al.* 2015), although in some cases, increases in synaptic strength have been observed (e.g. Power *et al.* 2016). We observed enhanced miniature synaptic amplitude, together with a reduction in miniature synaptic frequency, which suggests that the effects on synaptic transmission may be complex, especially given the changes in dendritic diameter that have previously been reported for these mice (Girard *et al.* 2012), which could have implication for dendritic filtering and synapse function. Interestingly, analysis of miniature rise times suggests that synapse location is not altered in *Sacs*$^{-/-}$ mice. One possible explanation for the complex regulation of synaptic strength could be homeo-static adaptive mechanisms (Turrigiano, 2017). In this scenario, Purkinje cells might respond to a reduction in the number of synaptic inputs (reflected by reduced frequency) by scaling up the strength of the remaining inputs (increased amplitude). Our analysis of the synaptic decay time constant suggests that subunit composition is unlikely to be changed by this upregulation of synaptic strength. Further studies will need to determine the
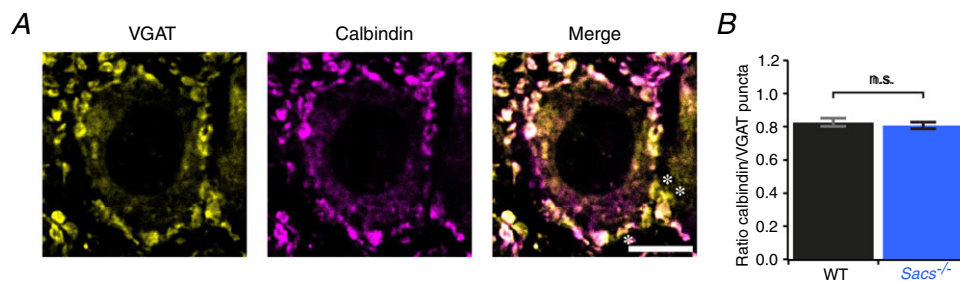

Figure 8. Ratio of Purkinje cell positive GABAergic puncta is high and unchanged in *Sacs*$^{-/-}$ DCN
A, representative images showing VGAT-positive GABAergic puncta (yellow, left) with calbindin-positive Purkinje-cell puncta (magenta, middle) apposed to a large DCN neuron, and merged image showing colabelled puncta (white, right) with occasional VGAT-positive, calbindin-negative puncta highlighted with asterisk. Scale bar, 15 μm. *B*, the proportion of calbindin-positive GABAergic puncta is high on WT DCN large neurons, and is unchanged in *Sacs*$^{-/-}$ DCN. $N = 4$ for both WT and *Sacs*$^{-/-}$; n.s., $P > 0.05$.

mechanistic impact that these changes have on Purkinje cell function and synaptic plasticity.

We observed changes in firing rate in Purkinje cells located in anterior, but not posterior, lobules at an age when motor deficits are observed (Lariviere *et al.* 2015), as well as weeks earlier prior to the detection of motor deficits. The regionalization of Purkinje cell deficits should impact the cerebellar-related impairments that are observed, although symptoms in ARSACS patients can be diverse, and no unique profile for ARSACS has
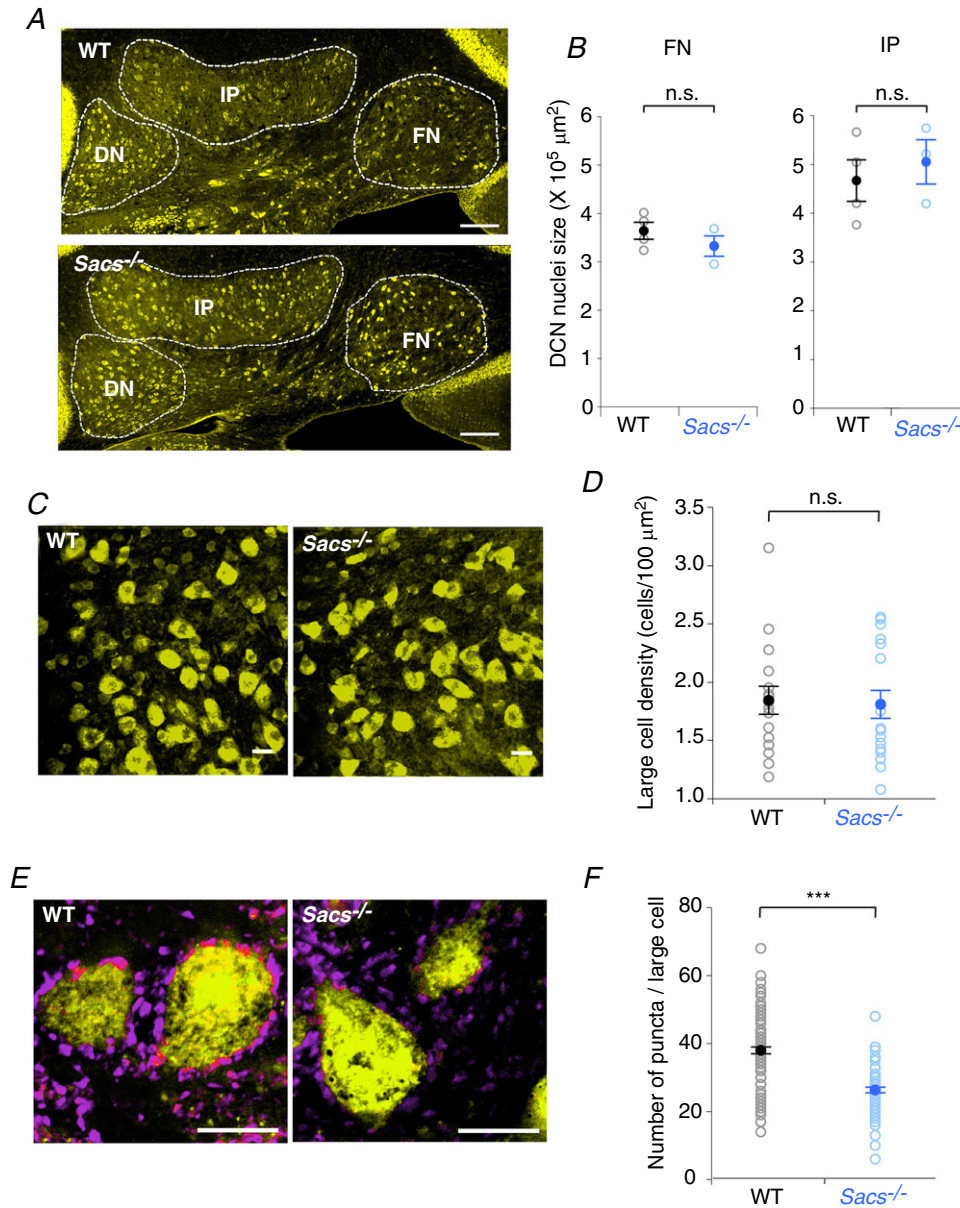
Figure 9. Reduction of Purkinje cell puncta on large neurons in the deep cerebellar nuclei (DCN) in *Sacs*$^{-/-}$ mice

A, representative images of deep cerebellar nuclei labelled with NeuN (yellow) with individual dentate (DN), fastigial (FN) and interposed (IN) nuclei indicated in dashed lines from WT (top) and *Sacs*$^{-/-}$ (bottom) mice. Scale bar, 200 μm. *B*, neither the FN (left) nor the IN (right) showed significant differences in volume in *Sacs*$^{-/-}$ mice ($N = 4$ for WT; $N = 3$ for *Sacs*$^{-/-}$ mice). *C*, representative image showing neurons labelled with NeuN (yellow) from WT (left) and *Sacs*$^{-/-}$ (right) mouse DCN. Only large neurons with >15 μm diameter were included for this and subsequent measurements. Scale bar, 15 μm. *D*, density of large-diameter cells was not significantly different in WT or *Sacs*$^{-/-}$ mice ($N = 4$ for WT and *Sacs*$^{-/-}$ mice). *E*, representative images showing Purkinje cell (calbindin-positive) puncta (magenta) on large cells (NeuN positive, yellow) in WT (left) and *Sacs*$^{-/-}$ (right) mouse DCN. Scale bar, 15 μm. *F*, the number of Purkinje cell positive puncta made onto DCN large cells was significantly reduced. WT: $N = 4$; *Sacs*$^{-/-}$: $N = 4$. n.s., $P > 0.05$; ***$P < 0.001$.

been described (Bouchard *et al.* 1978; Synofzik *et al.* 2013). There are other mouse models of ataxia that also predominantly affect anterior lobule Purkinje cells (e.g. Sawada *et al.* 2009; Sarna & Hawkes, 2011). It would be interesting to determine if these mice shared ataxic symptoms to a greater degree than in mouse models where cell loss was not regionally restricted, as this may shed light on functional regionalization in the cerebellum. Our observation that firing deficits occur only in anterior lobules where Purkinje cells later degenerate (Lariviere *et al.* 2015) supports the hypothesis that early firing deficits are part of the neurodegenerative process leading to later Purkinje cell loss. Evidence from other mouse models also appears to support this hypothesis: firing deficits prior to Purkinje cell loss have been observed in several animal models of ataxia (e.g. Walter *et al.* 2006; Shakkottai *et al.* 2009, 2011; Alviña & Khodakhah, 2010*a,b*; Hourez *et al.* 2011; Kasumu *et al.* 2012; Hansen *et al.* 2013; Dell'Orco *et al.* 2015; Mark *et al.* 2015; Jayabal *et al.* 2016), although the lobule-specific localization we observe in *Sacs*$^{-/-}$ mice is to our knowledge the first demonstration of regionalized firing deficits in an ataxia model. Whether rescuing Purkinje cell firing deficits would be sufficient to prevent later cell loss is currently unknown, but is a question of great clinical importance. Why are Purkinje cells in anterior lobules preferentially affected in ARSACS? Put another way, why are posterior Purkinje cells spared? Posterior lobule Purkinje cells already fire at lower frequencies than anterior Purkinje cells (Kim *et al.* 2012), which raises an alternative explanation that firing at lower frequencies is neuroprotective in *Sacs*$^{-/-}$ mice. If true, the reduction in firing deficits in anterior *Sacs*$^{-/-}$ Purkinje cells may itself be a homeostatic mechanism that opposes rather than contributes to later cell loss. It will be important to determine whether alterations in firing rate are causative or adaptive in mouse models of ataxia.

To our knowledge, our observation of synaptic and firing deficits in *Sacs*$^{-/-}$ mice is the first such observation in an autosomal recessive human ataxia model. Taken together with other studies, our findings suggest that common pathophysiological changes are observed in several ataxias caused by different genetic insults. It is possible that treatments targeted at firing and synaptic deficits may thus be a general means of treating diverse ataxias (Meera *et al.* 2016; Ady & Watt, 2017), a worthwhile goal since ataxias are rare diseases. Nonetheless, we observe several findings that must lead to caution. For instance, unlike in other mouse models (Inoue *et al.* 2001; Walter *et al.* 2006), we observed no changes in spike shape in *Sacs*$^{-/-}$ Purkinje cells, and low doses of 4-AP did not rescue firing deficits as they do in some (Inoue *et al.* 2001; Alviña & Khodakhah, 2010*b*; Hourez *et al.* 2011) but not all (Jayabal *et al.* 2016) mouse models. Even if firing deficits have different mechanistic underpinnings across ataxias,

however, it may still be possible to rescue firing and motor symptoms in several ataxias by a common treatment approach.

Finally, we observed a reduction in the number of Purkinje cell synapses made onto neurons in the DCN in *Sacs*$^{-/-}$ mice. This is interesting because DCN abnormalities have been observed in human patients with diverse forms of ataxia (Stefanescu *et al.* 2015), yet the DCN is not well studied in most ataxia models. Changes in DCN connectivity and cellular properties are likely to have profound effects on cerebellar function and disease progression, however, and should be studied further. One question raised by our observations is whether reduced Purkinje cell firing rates lead to a reduction in Purkinje cell puncta in the DCN, perhaps through Hebbian mechanisms (e.g. Kutsarova *et al.* 2016). How does reduced Purkinje cell innervation impact the DCN, and might other cellular abnormalities be observed? Sacsin is expressed in the DCN, and neurofilament accumulates in the DCN of *Sacs*$^{-/-}$ mice like in Purkinje cells (Lariviere *et al.* 2015), making it likely that other physiological alterations also occur in DCN neurons. Our finding of a reduction in Purkinje cell innervation of principal neurons of the DCN has the potential to profoundly impact cerebellar function, and merits further study. Our identification of synaptic and firing deficits in Purkinje cells adds to our growing understanding of the pathophysiology of ARSACS. A deeper understanding of these alterations is critical for the development of promising treatment strategies for this illness.

References

Ady V & Watt AJ (2017). New old drug(s) for spinocerebellar ataxias. *J Physiol* **595**, 5–6.

Alviña K & Khodakhah K (2010*a*). KCa channels as therapeutic targets in episodic ataxia type-2. *J Neurosci* **30**, 7249–7257.

Alviña K & Khodakhah K (2010*b*). The therapeutic mode of action of 4-aminopyridine in cerebellar ataxia. *J Neurosci* **30**, 7258–7268.

Arancillo M, White JJ, Lin T, Stay TL & Sillitoe RV (2015). In vivo analysis of Purkinje cell firing properties during postnatal mouse development. *J Neurophysiol* **113**, 578–591.

Bouchard JP, Barbeau A, Bouchard R & Bouchard RW (1978). Autosomal recessive spastic ataxia of Charlevoix-Saguenay. *Can J Neurol Sci* **5**, 61–69.

Bouchard JP, Richter A, Mathieu J, Brunet D, Hudson TJ, Morgan K & Melancon SB (1998). Autosomal recessive spastic ataxia of Charlevoix-Saguenay. *Neuromuscul Disord* **8**, 474–479.

Chang PK, Khatchadourian A, McKinney RA & Maysinger D (2015). Docosahexaenoic acid (DHA): a modulator of

microglia activity and dendritic spine morphology. *J Neuroinflammation* **12**, 34.

Chang PK, Prenosil GA, Verbich D, Gill R & McKinney RA (2014). Prolonged ampakine exposure prunes dendritic spines and increases presynaptic release probability for enhanced long-term potentiation in the hippocampus. *Eur J Neurosci* **40**, 2766–2776.

Dell'Orco JM, Wasserman AH, Chopra R, Ingram MA, Hu YS, Singh V, Wulff H, Opal P, Orr HT & Shakkottai VG (2015). Neuronal atrophy early in degenerative ataxia is a compensatory mechanism to regulate membrane excitability. *J Neurosci* **35**, 11292–11307.

De Zeeuw CI & Berrebi AS (1995). Postsynaptic targets of Purkinje cell terminals in the cerebellar and vestibular nuclei of the rat. *Eur J Neurosci* **7**, 2322–2333.

Duncan EJ, Lariviere R, Bradshaw TY, Longo F, Sgarioto N, Hayes MJ, Romano LEL, Nethisinghe S, Giunti P, Bruntraeger MB, Durham HD, Brais B, Maltecca F, Gentil BJ & Chapple JP (2017). Altered organization of the intermediate filament cytoskeleton and relocalization of proteostasis modulators in cells lacking the ataxia protein sacsin. *Hum Mol Genet* **26**, 3130–3143.

Engert JC, Berube P, Mercier J, Dore C, Lepage P, Ge B, Bouchard JP, Mathieu J, Melancon SB, Schalling M, Lander ES, Morgan K, Hudson TJ & Richter A (2000). ARSACS, a spastic ataxia common in northeastern Quebec, is caused by mutations in a new gene encoding an 11.5-kb ORF. *Nat Genet* **24**, 120–125.

Girard M, Lariviere R, Parfitt DA, Deane EC, Gaudet R, Nossova N, Blondeau F, Prenosil G, Vermeulen EG, Duchen MR, Richter A, Shoubridge EA, Gehring K, McKinney RA, Brais B, Chapple JP & McPherson PS (2012). Mitochondrial dysfunction and Purkinje cell loss in autosomal recessive spastic ataxia of Charlevoix-Saguenay (ARSACS). *Proc Natl Acad Sci U S A* **109**, 1661–1666.

Hansen ST, Meera P, Otis TS & Pulst SM (2013). Changes in Purkinje cell firing and gene expression precede behavioral pathology in a mouse model of SCA2. *Hum Mol Genet* **22**, 271–283.

Häusser M & Clark BA (1997). Tonic synaptic inhibition modulates neuronal output pattern and spatiotemporal synaptic integration. *Neuron* **19**, 665–678.

Hourez R, Servais L, Orduz D, Gall D, Millard I, de Kerchove d'Exaerde A, Cheron G, Orr HT, Pandolfo M & Schiffmann SN (2011). Aminopyridines correct early dysfunction and delay neurodegeneration in a mouse model of spinocerebellar ataxia type 1. *J Neurosci* **31**, 11795–11807.

Husson Z, Rousseau CV, Broll I, Zeilhofer HU & Dieudonne S (2014). Differential GABAergic and glycinergic inputs of inhibitory interneurons and Purkinje cells to principal cells of the cerebellar nuclei. *J Neurosci* **34**, 9418–9431.

Inoue T, Lin X, Kohlmeier KA, Orr HT, Zoghbi HY & Ross WN (2001). Calcium dynamics and electrophysiological properties of cerebellar Purkinje cells in SCA1 transgenic mice. *J Neurophysiol* **85**, 1750–1760.

Jayabal S, Chang HHV, Cullen KE & Watt AJ (2016). 4-aminopyridine reverses ataxia and cerebellar firing deficiency in a mouse model of spinocerebellar ataxia type 6. *Sci Rep* **6**, 29489.

Jayabal S, Ljungberg L, Erwes T, Cormier A, Quilez S, El Jaouhari S & Watt AJ (2015). Rapid onset of motor deficits in a mouse model of spinocerebellar ataxia type 6 precedes late cerebellar degeneration. *eNeuro* **2**, ENEURO.0094-15.2015.

Jayabal S, Ljungberg L & Watt AJ (2017). Transient cerebellar alterations during development prior to obvious motor phenotype in a mouse model of spinocerebellar ataxia type 6. *J Physiol* **595**, 949–966.

Kasumu AW, Hougaard C, Rode F, Jacobsen TA, Sabatier JM, Eriksen BL, Strobaek D, Liang X, Egorova P, Vorontsova D, Christophersen P, Ronn LC & Bezprozvanny I (2012). Selective positive modulator of calcium-activated potassium channels exerts beneficial effects in a mouse model of spinocerebellar ataxia type 2. *Chem Biol* **19**, 1340–1353.

Kim CH, Oh SH, Lee JH, Chang SO, Kim J & Kim SJ (2012). Lobule-specific membrane excitability of cerebellar Purkinje cells. *J Physiol* **590**, 273–288.

Kutsarova E, Munz M & Ruthazer ES (2016). Rules for shaping neural connections in the developing brain. *Front Neural Circuits* **10**, 111.

Lalanne T, Oyrer J, Mancino A, Gregor E, Chung A, Huynh L, Burwell S, Maheux J, Farrant M & Sjostrom PJ (2016). Synapse-specific expression of calcium-permeable AMPA receptors in neocortical layer 5. *J Physiol* **594**, 837–861.

Lariviere R, Gaudet R, Gentil BJ, Girard M, Conte TC, Minotti S, Leclerc-Desaulniers K, Gehring K, McKinney RA, Shoubridge EA, McPherson PS, Durham HD & Brais B (2015). Sacs knockout mice present pathophysiological defects underlying autosomal recessive spastic ataxia of Charlevoix-Saguenay. *Hum Mol Genet* **24**, 727–739.

Li X, Menade M, Kozlov G, Hu Z, Dai Z, McPherson PS, Brais B & Gehring K (2015). High-throughput screening for ligands of the HEPN domain of sacsin. *PLoS One* **10**, e0137298.

Mark MD, Krause M, Boele HJ, Kruse W, Pollok S, Kuner T, Dalkara D, Koekkoek S, De Zeeuw CI & Herlitze S (2015). Spinocerebellar ataxia type 6 protein aggregates cause deficits in motor learning and cerebellar plasticity. *J Neurosci* **35**, 8882–8895.

Mark MD, Maejima T, Kuckelsberg D, Yoo JW, Hyde RA, Shah V, Gutierrez D, Moreno RL, Kruse W, Noebels JL & Herlitze S (2011). Delayed postnatal loss of P/Q-type calcium channels recapitulates the absence epilepsy, dyskinesia, and ataxia phenotypes of genomic *Cacna1a* mutations. *J Neurosci* **31**, 4311–4326.

Martin MH, Bouchard JP, Sylvain M, St-Onge O & Truchon S (2007). Autosomal recessive spastic ataxia of Charlevoix-Saguenay: a report of MR imaging in 5 patients. *AJNR Am J Neuroradiol* **28**, 1606–1608.

McKay BE & Turner RW (2005). Physiological and morphological development of the rat cerebellar Purkinje cell. *J Physiol* **567**, 829–850.

Meera P, Pulst SM & Otis TS (2016). Cellular and circuit mechanisms underlying spinocerebellar ataxias. *J Physiol* **594**, 4653–4660.

Napper RM & Harvey RJ (1988). Number of parallel fiber synapses on an individual Purkinje cell in the cerebellum of the rat. *J Comp Neurol* **274**, 168–177.

Ouyang Y, Takiyama Y, Sakoe K, Shimazaki H, Ogawa T, Nagano S, Yamamoto Y & Nakano I (2006). Sacsin-related ataxia (ARSACS): expanding the genotype upstream from the gigantic exon. *Neurology* **66**, 1103–1104.

Parfitt DA, Michael GJ, Vermeulen EG, Prodromou NV, Webb TR, Gallo JM, Cheetham ME, Nicoll WS, Blatch GL & Chapple JP (2009). The ataxia protein sacsin is a functional co-chaperone that protects against polyglutamine-expanded ataxin-1. *Hum Mol Genet* **18**, 1556–1565.

Person AL & Raman IM (2012). Purkinje neuron synchrony elicits time-locked spiking in the cerebellar nuclei. *Nature* **481**, 502–505.

Power EM, Morales A & Empson RM (2016). Prolonged type 1 metabotropic glutamate receptor dependent synaptic signaling contributes to spino-cerebellar ataxia type 1. *J Neurosci* **36**, 4910–4916.

Sarna JR & Hawkes R (2011). Patterned Purkinje cell loss in the ataxic sticky mouse. *Eur J Neurosci* **34**, 79–86.

Sawada K, Kalam Azad A, Sakata-Haga H, Lee NS, Jeong YG & Fukui Y (2009). Striking pattern of Purkinje cell loss in cerebellum of an ataxic mutant mouse, tottering. *Acta Neurobiol Exp (Wars)* **69**, 138–145.

Scoles DR, Meera P, Schneider MD, Paul S, Dansithong W, Figueroa KP, Hung G, Rigo F, Bennett CF, Otis TS & Pulst SM (2017). Antisense oligonucleotide therapy for spinocerebellar ataxia type 2. *Nature* **544**, 362–366.

Shakkottai VG, do Carmo Costa M, Dell'Orco JM, Sankaranarayanan A, Wulff H & Paulson HL (2011). Early changes in cerebellar physiology accompany motor dysfunction in the polyglutamine disease spinocerebellar ataxia type 3. *J Neurosci* **31**, 13002–13014.

Shakkottai VG, Xiao M, Xu L, Wong M, Nerbonne JM, Ornitz DM & Yamada KA (2009). FGF14 regulates the intrinsic excitability of cerebellar Purkinje neurons. *Neurobiol Dis* **33**, 81–88.

Shuvaev AN, Hosoi N, Sato Y, Yanagihara D & Hirai H (2017). Progressive impairment of cerebellar mGluR signalling and its therapeutic potential for cerebellar ataxia in spinocerebellar ataxia type 1 model mice. *J Physiol* **595**, 141–164.

Sjostrom PJ & Hausser M (2006). A cooperative switch determines the sign of synaptic plasticity in distal dendrites of neocortical pyramidal neurons. *Neuron* **51**, 227–238.

Stefanescu MR, Dohnalek M, Maderwald S, Thurling M, Minnerop M, Beck A, Schlamann M, Diedrichsen J, Ladd ME & Timmann D (2015). Structural and functional MRI abnormalities of cerebellar cortex and nuclei in SCA3, SCA6 and Friedreich's ataxia. *Brain* **138**, 1182–1197.

Synofzik M, Soehn AS, Gburek-Augustat J, Schicks J, Karle KN, Schule R, Haack TB, Schoning M, Biskup S, Rudnik-Schoneborn S, Senderek J, Hoffmann KT, MacLeod P, Schwarz J, Bender B, Kruger S, Kreuz F, Bauer P & Schols L (2013). Autosomal recessive spastic ataxia of Charlevoix Saguenay (ARSACS): expanding the genetic, clinical and imaging spectrum. *Orphanet J Rare Dis* **8**, 41.

Thiffault I, Dicaire MJ, Tetreault M, Huang KN, Demers-Lamarche J, Bernard G, Duquette A, Lariviere R, Gehring K, Montpetit A, McPherson PS, Richter A, Montermini L, Mercier J, Mitchell GA, Dupre N, Prevost C, Bouchard JP, Mathieu J & Brais B (2013). Diversity of ARSACS mutations in French-Canadians. *Can J Neurol Sci* **40**, 61–66.

Turrigiano GG (2017). The dialectic of Hebb and homeostasis. *Philos Trans R Soc Lond B Biol Sci* **372**, 20160258.

Voogd J (2011). Cerebellar zones: a personal history. *Cerebellum* **10**, 334–350.

Walter JT, Alvina K, Womack MD, Chevez C & Khodakhah K (2006). Decreases in the precision of Purkinje cell pacemaking cause cerebellar dysfunction and ataxia. *Nat Neurosci* **9**, 389–397.

Watt AJ, Cuntz H, Mori M, Nusser Z, Sjöström PJ & Häusser M (2009). Traveling waves in developing cerebellar cortex mediated by asymmetrical Purkinje cell connectivity. *Nat Neurosci* **12**, 463–473.

Additional information

Competing interests

The authors declare no competing interests or conflicts of interests.

Author contributions

V.A. and B.T.M. acquired, analysed and interpreted the data and contributed to drafting and editing the manuscript. M.N., P.C., J.H., A.C. and F.C. acquired, analysed and interpreted data. R.L and B.B. provided mice and contributed to drafting and editing the manuscript. R.A.M. and A.J.W. conceived of and designed the work, analysed and interpreted the data, and drafted and edited the manuscript. All authors agree to be accountable for all aspects of the work in ensuring that questions related to the accuracy or integrity of any part of the work are appropriately investigated and resolved. All persons listed as authors qualify for authorship and all those who qualify are listed.